COMMUNICATION

CrossMark
← click for updates

Improved H$_2$S gas sensing properties of ZnO nanorods *via* decoration of nano-porous SiO$_2$ thin layers†

Gaocan Qi,‡[ab] Xiaodan Lu‡[a] and Zhihao Yuan*[ab]

Oriented ZnO nanorods are successfully decorated with a thin layer of nano-porous SiO$_2$ film *via* solution method. The as-prepared ZnO@SiO$_2$ composite nanostructure displays superior stability for the detection of a low concentration H$_2$S. A molecule-isolation mechanism is suggested to interpret the improved H$_2$S sensing properties of the ZnO@SiO$_2$ composite nanostructure.

Metal oxide nanomaterials,[1–3] such as SnO$_2$, ZnO, NiO, MoO$_3$, WO$_3$ *etc.*, have been widely used for the detection of inflammable and toxic gases in ambient air because of their large specific surface, low cost, facial fabrication and high compatibility with the microelectronic fabrication process. Metal oxide sensors (MOS) manifest advantages of high sensitivity, fast response and wide working temperature in detection of hazardous gases. However, the application of MOS still faces a serious problem of poisoning in detecting acidic gases, especially hydrogen sulfide (H$_2$S).[4–7] In addition, the instability of MOS over prolonged usage is also attributed to the poisoning process.[8] Hence, improving the stability of MOS in H$_2$S detection is of great importance in the design of sensing devices.

In recent years, many efforts have been devoted to prevent H$_2$S poisoning by modifying metal oxides with chemically inactive materials. Kohl *et al.* and Bai *et al.* reported graphene–ZnO[9] and reduced graphene oxide (rGo)–MoO$_3$[10] hybrid-materials for stable detection of H$_2$S with sensitivity of only 0.25 to 2 ppm H$_2$S and less than 5 to 5 ppm H$_2$S. Kumar and co-workers[11] modified ZnO nanowires with different thickness of cobalt phthalocyanine (CoPc) to increase its stability for H$_2$S detection. The heterojunction films prepared with a 25 nm thick CoPc layer exhibited the highest response of 2.68 to 10 ppm H$_2$S. Unfortunately, the modification of inert materials

significantly reduced the sensitivity of metal oxides to H$_2$S, which is not suit to monitor low concentration H$_2$S (*e.g.* ppm- or ppb-level). In our previous work,[12] we decorated ZnO nanorods with a several nm ZnS layer to improve the H$_2$S gas sensing properties. The as-prepared sensor showed satisfactory stability, sensitivity and selectivity for detection of ppm-level H$_2$S at room temperature. But, the surface ZnS thin layer is not stable when it was used at high working temperature. Hence, design and fabrication of stable and sensitive H$_2$S sensor with metal oxides is still a challenge in the present researches.

Here in, we envision that a porous thin film of chemical inactive materials with nano-holes on metal oxide nanostructure may improve its stability and keep its high sensitivity, because the inactive film is able to prevent the contact between metal oxides and H$_2$S, while the nano-holes allow the penetration of electrons for formation of chemisorbed oxygen layer. To verify this design, we modified ZnO nanorods with a thin layer of porous SiO$_2$ *via* solution route. The ZnO@SiO$_2$ nanostructure presents a stable detection of H$_2$S down to ppb level at room temperature. In addition, the as-prepared sensing device is capable of steadily working at 300 °C.

Oriented ZnO nanorods were grown on flat ceramic substrate with interdigitated electrodes *via* a two-step solution approach. The detailed growth processes were described in our previous work.[12] For the modification of ZnO nanorods with SiO$_2$ film, the as-prepared samples were immersed in freshly prepared 0.0125 mmol L^{-1} 3-aminopropyl triethoxysilane (APS) aqueous solution, followed by adding 32 mL sodium silicate (Na$_2$SiO$_3$) aqueous solution (0.54% (wt/wt)) and adjusting the pH to 10.8 with hydrochloric acid.[13,14] After stirring for 3 min at room temperature, the mixed solution was heated in a 90 °C water bath for different lengths of time (0–80 min). Finally, the reaction was stopped by placing hot solution in an ice bath, and the resulting products were rinsed with deionized water and dried at 60 °C.

The morphology and structure of the samples were characterized by field-emission scanning electron microscopy (FE-SEM, JEOL JSM-6700F) and transmission electron microscopy

aSchool of Materials Science and Engineering, Tianjin University of Technology, Tianjin 300384, China. E-mail: zhyuan@tjut.edu.cn

bTianjin Key Lab for Photoelectric Materials & Devices, Tianjin 300384, China

‡ These authors contributed equally to the work.

(TEM, JEOL JEM-2100). Energy dispersive spectrometer (EDS, Oxford) was used to analyze the chemical components of the as-prepared samples. Gas sensing tests were performed with a CGS-1TP intelligent gas sensitive analysis system (Beijing Alice Technology Co., Ltd, China) using a stationary state gas distribution method. H₂S was diluted to 4000 ppm with dry nitrogen, and then injected into the test chamber by micro-injector.

The sensor's sensitivity to the test gas (S_r) is defined as follows:

$$S_r = R_a/R_g$$

where R_a is the resistance of the sensor in air, and R_g is the resistance in a test gas.

A layer of densely packed and oriented ZnO nanorods grows on the ceramic substrate between the interdigital Au electrodes *via* two-step solution approach (Fig. 1a and b). The diameters of rod-like ZnO structure are 80–100 nm and the average length of nanorods is about 1.2 μm (cross-section image and XRD pattern of as-grown ZnO nanorods are shown in Fig. S1†). Fig. 1c–f presents the morphology-evolution of as-grown ZnO nanorods immersed in APS–Na₂SiO₃ solution at 90 °C for different time. The distinct lattice fringe in Fig. 1c demonstrates that the rod-like nanostructure is well crystalline ZnO crystal without impurities. After immersion in APS–Na₂SiO₃ solution at 90 °C

for 20 min, some plausible amorphous substances can be seen on the rod-like nanostructure, which is marked with arrows (Fig. 1d). When immersed for 40 min, the lattice fringe of the nanorod becomes obscure but still distinct at some patches marked with irregular red circles (Fig. 1e). This result implies that the nanorod's surface is covered by a layer porous amorphous material, and the holes of porous film have diameters about 2–4 nm. Corresponding EDS data shown in Fig. S2† confirms that the porous coating is composed of amorphous SiO₂. When the reaction time is prolonged to 80 min, a continuous amorphous film is form on the ZnO nanorod with thickness of about 1–2 nm (see low magnification TEM image in Fig. S3†). As a consequence, lattice fringe of ZnO crystal just can be seen at a special part near the edge of rod (Fig. 1f).

The sensing behaviour of pure ZnO nanorods and ZnO@SiO₂ composite nanostructure towards H₂S at room temperature is summarized in Fig. 2. As is shown in Fig. 2a, the response of oriented ZnO nanorods to 10 ppm H₂S is as high as 1180, but the response curve cannot recover to the original baseline. The top-right inset of Fig. 2a shows that the response resistance of ZnO nanorod-based device recovers not more than 5% of the base value and reaches a new baseline. This irrecoverable response of ZnO nanorod-based device ought to be attributed to the irreversible chemical reaction between H₂S and the ZnO nanorod,[15,16] in which ZnS is formed on the surface.

To prevent the reaction between ZnO and H₂S, we modified the as-grown ZnO nanorods with chemical inactive SiO₂ film by hydrolysis method. Fig. 2b and top-right inset show that the sensitivity of oriented ZnO nanorods, treated in APS–Na₂SiO₃ solution at 90 °C for 20 min, decreases to about 210 and the response resistance recovers to about 50% of original value. When a porous SiO₂ thin film forms on ZnO nanorods, the ZnO@SiO₂ composite nanostructure shows a recoverable response for detection of 10 ppm H₂S with a sensitivity of 116 (Fig. 2c). Its response and recovery times are 200 s and 600 s, respectively. With further increase of SiO₂ thickness, the
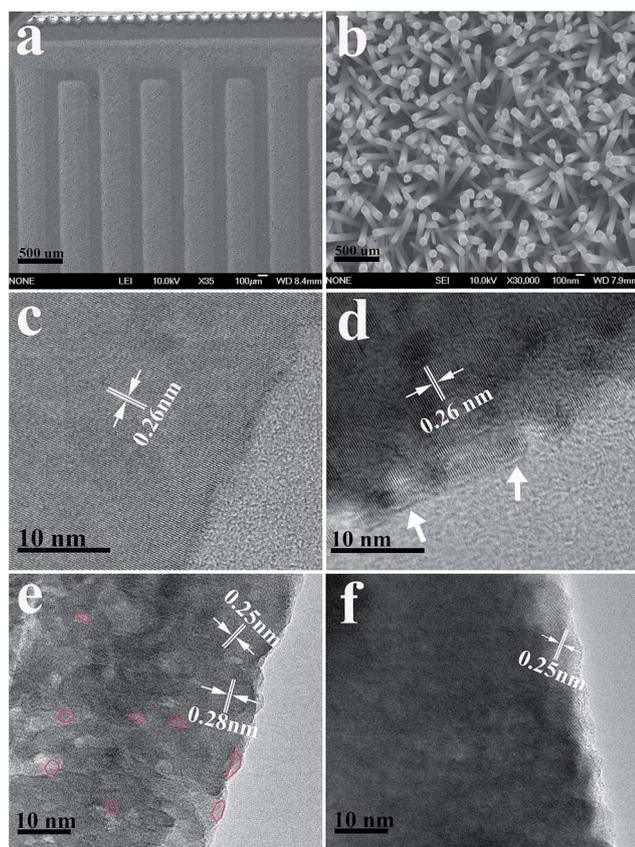
Fig. 1 FE-SEM images of interdigital electrodes (a) and the as-grown ZnO nanorods (b). TEM images of ZnO nanorods immersed in APS–Na₂SiO₃ solution at 90 °C for different time. (c) 0 min; (d) 20 min; (e) 40 min; (f) 80 min.
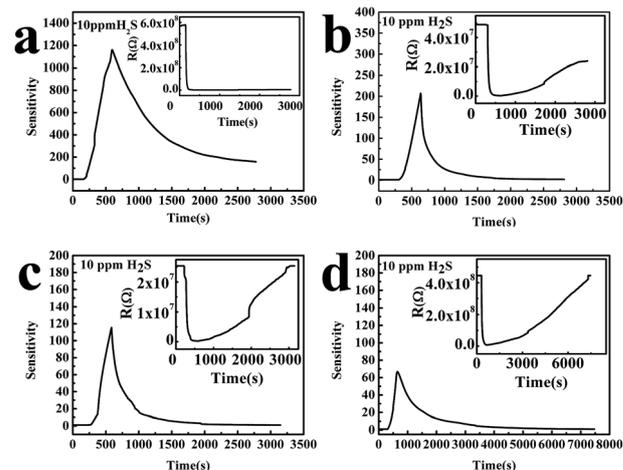
Fig. 2 The H₂S sensing behaviour of ZnO nanorods (a) and ZnO–SiO₂ composite nanostructure (b–d) prepared in APS–Na₂SiO₃ solution at 90 °C for 20, 40 and 80 minutes. The top-right insets show the corresponding resistance variation of as-prepared sensors.

response of ZnO@SiO$_2$ composite nanostructure is still capable of recovery, but the recovery time is prolonged to 3000 s (Fig. 2d). These results demonstrate that porous SiO$_2$ film improves the recovery behaviour of ZnO nanorod-based sensor for H$_2$S detection, but a thick film prolongs its recovery time. Hence, the sample treated in APS–Na$_2$SiO$_3$ solution at 90 °C for 40 min displays the optimum sensing properties.

The ZnO@SiO$_2$ composite nanostructure shown in Fig. 1e has the potential of stable detection of lower concentration H$_2$S, because its sensitivity of 116 to 10 ppm gas is a relatively high value. Its sensing properties to low concentration H$_2$S, less than 1 ppm, were tested in our experiment. Fig. 3 shows five time-cycling response of the sensor for each concentration. It can be seen that the sensitivities of as-prepared sensor don't change too much in the five time-cycling. The average sensitivities are 1.30, 2.67, 3.28 and 11.28 to 25 ppb, 100 ppb, 500 ppb and 1 ppm H$_2$S, respectively. The deviations of sensitivities to each concentration are less than 1%. These results demonstrate that the ZnO@SiO$_2$ composite nanostructure has good reusability for the detection of ppb level H$_2$S.

The stability of as-prepared sensors at different working temperature was also tested in this work. Fig. 4 shows the sensing behaviour of ZnO@SiO$_2$ composite nanostructure (shown in Fig. 1c) to 1 ppm H$_2$S at 150 °C and 300 °C, respectively. It can be seen that the sensitivities of as-prepared sensor
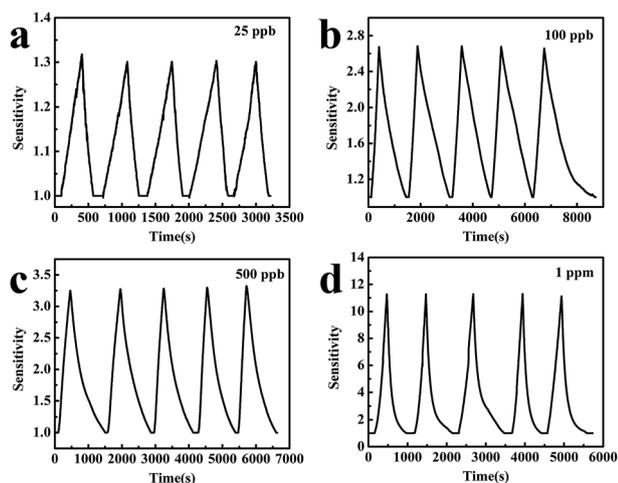
increase slightly with the increase of working temperature. The response of as-prepared sensor displays a stable sensing behaviour at each working temperature. It is worth to note that the response and recovery time decrease to 60 s and 80 s, respectively, at 300 °C. These results show that the sensor can be steadily utilized at working temperature range of 25–300 °C without structure instability.

Fig. 5 shows response of the sensor based on ZnO@SiO$_2$ composite nanostructure to several reducing gases at room temperature. We can see that the sensor displays a high sensitivity to 10 ppm H$_2$S but small sensitivities to other reducing gases even in the case of very high concentration. The sensitivities are not more than 2 for 5000 ppm formaldehyde, ethanol, and hydrogen. This result clearly shows that the sensor based on ZnO@SiO$_2$ composite nanostructure possesses satisfactory selectivity for the detection of H$_2$S. This superior selectivity of the sensor should be owed to the high reactivity between H$_2$S and O$_2$ at room temperature.

Having taken into account the above results and discussion of TEM images and sensing behaviours, a tentative molecule-isolation mechanism is proposed to interpret the stability of ZnO@SiO$_2$ composite nanostructure for detecting H$_2$S. When the ZnO nanorod is bare, H$_2$S molecules reach and react with ZnO surface easily[17] (Fig. 6a), since absorbed oxygen layer on ZnO nanorod is thin at room temperature. Porous SiO$_2$ thin film improves the H$_2$S sensing property of ZnO nanorods by isolating ZnO surface from ambient H$_2$S molecules (Fig. 6b). On the one hand, the SiO$_2$ film can prevent the contact between H$_2$S molecules and ZnO nanorod, because it is chemically inert to

Fig. 3 Stability tests of ZnO@SiO$_2$ composite nanostructure (shown in Fig. 1e) to different H$_2$S concentrations.

Fig. 4 The stability of ZnO@SiO$_2$ composite nanostructure for detection of 1 ppm H$_2$S at different working temperature.
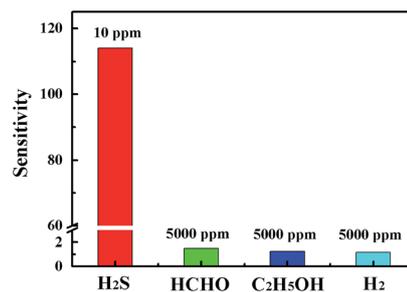
Fig. 5 Selectivity of ZnO@SiO$_2$ composite nanostructure to several reducing gases at room temperature.
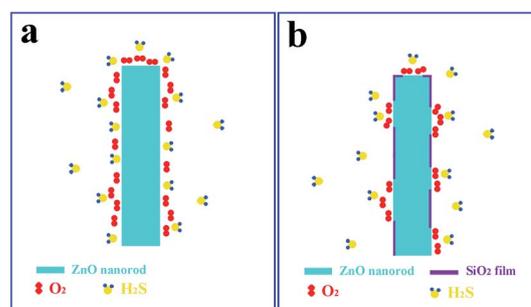
Fig. 6 Schematic representation of sensing mechanism of bare ZnO nanorod (a) and ZnO@SiO$_2$ composite nanostructure (b) for detecting H$_2$S.

H_2S. On the other hand, electrons in conduction band of ZnO are still capable of passing from the nanoscale holes of porous film to adsorbed oxygen molecule, forming chemisorbed oxygen layer.[18] Although, the observed diameters (2–4 nm) of holes on porous SiO_2 film are greater than H_2S molecule's diameter, the hole structure increases the stability of adsorbed oxygen layer. In addition, the exposed ZnO surface in nano-holes might be covered with picometer-scale porous SiO_2 thin film, which can't be observed by TEM. Hence, the surface modification of SiO_2 porous film effectively prevents the reaction between ZnO and H_2S, and retains the high sensitivity of ZnO nanorod. The stable response of ZnO@SiO_2 composite nanostructure at elevated working temperature benefits from the thermostability of SiO_2 materials.

We have demonstrated a strategy of modifying ZnO nanorods by a thin layer of porous SiO_2 for improving H_2S sensing properties. Under optimum conditions, the sensor based on ZnO@SiO_2 composite nanostructure gives a satisfactory stability for the detection of low concentration H_2S, even in the case of 25 ppb. The as-prepared sensor still has a stable response to H_2S at elevated working temperature. These superior properties are especially useful for detecting H_2S in air ambience. A molecule-isolation mechanism is suggested to explain the improvement of H_2S sensing properties. Furthermore, the decoration of nano-porous chemical inert materials might be used to improve H_2S sensing properties of other metal oxides.

Acknowledgements

Notes and references

1 K. Wetchakun, T. Samerjai, N. Tamaekong, C. Liewhiran, C. Siriwong, V. Kruefu, A. Wisitsoraat, A. Tuantranont and S. Phanichphant, *Sens. Actuators, B*, 2011, **160**, 580–591.

2 G. Korotcenkov, *Sens. Actuators, B*, 2005, **107**, 209–232.

3 W. Guo, L. Mei, J. Wen and J. Ma, *RSC Adv.*, 2016, **6**, 15048–15053.

4 D. D. Vuong, G. Sakai, K. Shimanoe and N. Yamazoe, *Sens. Actuators, B*, 2005, **105**, 437–442.

5 D. Fu, C. Zhu, X. Zhang, C. Li and Y. Chen, *J. Mater. Chem. A*, 2016, **4**, 1390–1398.

6 T. Yu, X. Cheng, X. Zhang, L. Sui, Y. Xu, S. Gao, H. Zhao and L. Huo, *J. Mater. Chem. A*, 2015, **3**, 11991–11999.

7 L. Yin, D. Chen, M. Feng, L. Ge, D. Yang, Z. Song, B. Fan, R. Zhang and G. Shao, *RSC Adv.*, 2015, **5**, 328–337.

8 G. Korotcenkov and B. K. Cho, *Sens. Actuators, B*, 2011, **156**, 527–538.

9 T. V. Cuong, V. H. Pham, J. S. Chung, E. W. Shin, D. H. Yoo, S. H. Hahn, J. S. Huh, G. H. Rue, E. J. Kim, S. H. Hur and P. A. Kohl, *Mater. Lett.*, 2010, **64**, 2479–2482.

10 S. Bai, C. Chen, M. Cui, R. Luo, A. Chen and D. Li, *RSC Adv.*, 2015, **5**, 50783–50789.

11 A. Kumar, S. Samanta, A. Singh, M. Roy, S. Singh, S. Basu, M. M. Chehimi, K. Roy, N. Ramgir, M. Navaneethan, Y. Hayakawa, A. K. Debnath, D. K. Aswal and S. K. Gupta, *ACS Appl. Mater. Interfaces*, 2015, **7**, 17713–17724.

12 G. Qi, L. Zhang and Z. Yuan, *Phys. Chem. Chem. Phys.*, 2014, **16**, 13434–13439.

13 J. F. Li, X. D. Tian, S. B. Li, J. R. Anema, Z. L. Yang, Y. Ding, Y. F. Wu, Y. M. Zeng, Q. Z. Chen, B. Ren, Z. L. Wang and Z. Q. Tian, *Nat. Protoc.*, 2013, **8**, 52–65.

14 J. F. Li, Y. F. Huang, Y. Ding, Z. L. Yang, S. B. Li, X. S. Zhou, F. R. Fan, W. Zhang, Z. Y. Zhou, Y. Wu de, B. Ren, Z. L. Wang and Z. Q. Tian, *Nature*, 2010, **464**, 392–395.

15 L. Ling, J. Wu, J. Song, P. Han and B. Wang, *Comput. Theor. Chem.*, 2012, **1000**, 26–32.

16 Z. Liu, T. Fan, D. Zhang, X. Gong and J. Xu, *Sens. Actuators, B*, 2009, **136**, 499–509.

17 K. J. Iversen and M. J. S. Spencer, *J. Phys. Chem. C*, 2013, **117**, 26106–26118.

18 G. Qi, S. Zhao and Z. Yuan, *Sens. Actuators, B*, 2013, **184**, 143–149.